Title: Homeostatic remodeling of mammalian membranes in response to dietary lipids is essential for cellular fitness

Short title: Homeostasis of mammalian membranes

Authors: Kandice R Levental*, Eric Malmberg, Yang-Yi Fan, Robert Chapkin, Robert Ernst, Ilya Levental*

Authors affiliations: Kandice R Levental[a], Eric Malmberg[a], Yang-Yi Fan[b], Robert Chapkin[b], Robert Ernst[c], Ilya Levental[a]

[a]University of Texas Health Science Center at Houston, Houston, TX, USA

[b]Program in Integrative Nutrition & Complex Diseases and Department of Nutrition & Food Science, Texas A&M University, College Station, TX, USA.

[c]Department of Medical Biochemistry and Molecular Biology, Medical Faculty, Saarland University, 66421 Homburg, Germany

***Co-corresponding authors:** Dr. Ilya Levental and Dr. Kandice Levental

Address: Suite 4.202A, 6431 Fannin St, Houston, TX, USA 77030

Phone: +1–713–500–5566

Fax: +1–713–500–7456

Email: ilya.levental@uth.tmc.edu ; kandice.r.levental@uth.tmc.edu

Keywords: membrane fluidity, lipidomics, diet, homeostasis, adaptation, saturated lipid, polyunsaturated fatty acid, cholesterol, SREBP

ABSTRACT

Biological membranes form the functional, dynamic interface that hosts a major fraction of all cellular bioactivity. Proper membrane physiology requires maintenance of a narrow range of physicochemical properties, which must be buffered from external perturbations. While homeostatic adaptation of membrane fluidity to temperature variation is a ubiquitous design feature of ectothermic organisms, such responsive membrane adaptation to external inputs has not been directly observed in mammals. Here, we report that challenging mammalian membrane homeostasis by dietary lipids leads to robust lipidomic remodeling to preserve membrane physical properties. Specifically, exogenous polyunsaturated fatty acids (PUFAs) are rapidly and extensively incorporated into membrane lipids, inducing a reduction in membrane packing. These effects are rapidly compensated both in culture and *in vivo* by lipidome-wide remodeling, most notably upregulation of saturated lipids and cholesterol. These lipidomic changes result in recovery of membrane packing. This lipidomic and biophysical compensation is centrally mediated by the sterol regulatory machinery, whose pharmacological or genetic abrogation results in decreased cellular fitness when membrane homeostasis is challenged by dietary lipids. These results reveal an essential mammalian mechanism for membrane homeostasis wherein lipidome remodeling in response to dietary lipid inputs preserves functional membrane phenotypes.

INTRODUCTION

Lipidic membranes are the essential barriers between life and the abiotic world and also mediate most intracellular compartmentalization in eukaryotic cells. However, the role of membranes is not limited to passive barriers. Approximately one third of all proteins are membrane-embedded [1], and many more are membrane-associated through post-translational modifications, lipid binding, and protein-protein interactions. Thus, a major fraction of cellular bioactivity occurs at membrane interfaces. Importantly, the physicochemical properties of the lipid matrix are key contributors to membrane physiology. A canonical example is membrane viscosity, which determines protein diffusivity, and thus protein-protein interaction frequency. Another is membrane permeability, which governs the diffusion of solutes into and out of the cytosol. Numerous other membrane physical parameters can determine protein behavior, including but not limited to fluidity, permeability, curvature, tension, packing, bilayer thickness, and lateral compartmentalization [2-12].

Because of their central role in protein function, effective maintenance of membrane properties is essential for survival in a complex and variable environment. In ectothermic (i.e. non-thermoregulating) organisms,

a pervasive challenge to membrane homeostasis comes in the form of temperature variations. Low temperature reduces the motion of lipid acyl chains, causing membranes to laterally contract, stiffen, and become more viscous [13]. Organisms across the tree of life, from prokaryotes to ectothermic animals, respond to such perturbations by tuning membrane lipid composition, down-regulating tightly packing lipids (e.g. containing saturated acyl chains) and up-regulating more loosely packed ones containing unsaturations or methylations in their lipid tails [13-15]. This response was termed 'homeoviscous adaptation', as these lipid changes result in remarkable constancy in membrane fluidity in spite of variable growth conditions [13,14,16]. It is worth noting that while fluidity is maintained at a specific set point, it should not be assumed that this is either the control variable, or the physical property being sensed; rather membrane fluidity may correlate with other membrane/lipid control parameters. For example, membrane homeostasis in *Bacillus subtilis* is mediated by the DesK sensor that is believed to sense membrane thickness [17]. In the yeast endoplasmic reticulum (ER), recently discovered sensors are sensitive specifically to lipid packing [5] and bilayer compressibility [18].

Excepting a few specialized instances (e.g. hibernation), mammals and other warm-blooded animals are not subject to large-scale variations in body temperature; thus, there has been relatively little investigation of homeostatic membrane responsiveness in such organisms. However, it is a well-established but under-appreciated fact that mammalian membrane homeostasis is extensively challenged by dietary inputs. Dietary lipids have major impacts on membrane compositions *in vivo* [19,20], and these perturbations must presumably be buffered to maintain cellular functionality. Mammalian lipidomes are much more complex [21-23] than either bacteria [24] or yeast [25,26], suggesting more potential control nodes required to balance the various conflicting demands of mammalian membrane physiology.

The possibility of a homeoviscous response in mammalian cells was suggested by two studies in the 1970s, which used a spontaneously arising mutant of Chinese Hamster Ovary (CHO) cells that is defective in cholesterol regulation [27,28]. These mutants accumulate cholesterol compared to wild-type CHO cells, but maintain normal membrane fluidity, possibly through modulation of their phospholipid profiles. However, the molecular etiology of the defects in these mutants remains unknown, and it was not reported where the cholesterol in these cells was accumulating (possibly storage organelles or lysosomes). Further, limitations of then-available technologies prevented direct demonstration of lipidomic responses to cholesterol modulation. Thus, the relevance of those insights to physiologically relevant perturbations of metabolically normal mammalian cells remains unclear. More recently, homeoviscous adaptation in mammals has been inferred from data-driven modeling approaches, which used the physical properties (melting temperature, intrinsic curvature) of pure lipids to extrapolate those of complex, biological

membranes [29,30]. However, the inherent non-additivity [31] and non-ideality [32] of lipid mixtures suggests that extrapolation of physical parameters of complex membranes from pure lipids may not be a reliable approach. Finally, lipid composition and membrane properties have been implicated in the heat shock response, though usually with a specific focus on signaling in the proteostasis network [33].

Here, we directly evaluate the hypothesis that mammalian membranes homeostatically adapt to dietary inputs by characterizing the lipidomic and biophysical responses to dietary fatty acids in several mammalian cell types and *in vivo*. We show that polyunsaturated fatty acids (PUFAs) are robustly incorporated into membrane phospholipids, introducing significant biophysical perturbations. This perturbation is counterbalanced by nearly concomitant lipidomic remodeling, most notable in the upregulation of saturated lipids and cholesterol. This remodeling normalizes membrane biophysical properties. These responses are centrally mediated by transcriptional sterol-regulatory machinery involving the Sterol Regulatory Element Binding Protein SREBP2. Finally, we show that the homeostatic membrane response is essential for cellular fitness, as abrogation of key response nodes leads to cytotoxic effects when membrane homeostasis is challenged by exogenous fatty acids.

RESULTS

Robust and specific incorporation of PUFAs into membrane lipids

Recent observations revealed that supplementation of cultured mammalian mast cells (rat basophilic leukemia cells (RBL)) with docosahexaenoic acid (DHA) leads to robust incorporation of this dietary polyunsaturated fatty acid into membrane lipids [23]. We observed similar effects in isolated human mesenchymal stem cells [34], cultured Chinese hamster ovary (CHO) cells, and rat primary hippocampal neurons (Supp Fig S1), confirming that uptake and incorporation of exogenous DHA into membrane lipids is not cell-type specific. Supplementation designed to recapitulate DHA-enriched diets in mammals (see Materials and Methods) increased the fraction of DHA-containing glycerophospholipids (GPLs) by nearly 15-fold (from <1 to ~15 mol%) (Fig 1A). Similarly, supplementation with the more common PUFA ω-6 arachidonic acid (AA) increased the fraction of AA-containing lipids by >3-fold (Fig 1B). Surprisingly, supplementation with monounsaturated (oleic; OA) acid or saturated (palmitic; PA) fatty acid produced only minimal lipidomic changes (Supp Fig S2). We speculate that this disparity in incorporation between PUFAs and more saturated FAs is associated with their availability in cell culture media: cells have access to sufficient levels of OA and PA such that supplementation has no effect, whereas PUFA levels are

limited such that supplementation with the physiologically appropriate concentrations used here leads to robust uptake and incorporation.

To confirm that the membrane incorporation of supplemented PUFAs in cultured cells appropriately recapitulates *in vivo* conditions, we analyzed the membrane lipidomes of mouse hearts and livers after two weeks of free-feeding on chow containing either fish oil (FO; 22.5% w-3 PUFAs, detailed fatty acid composition in Supplement) or corn oil (CO; 1.3% w-3 PUFAs), as previously described[35]. Consistent with previous observations[35-37] and the *in vitro* measurements here, dietary fish oil supplementation produced a robust incorporation of DHA into membrane lipids, with ~3-fold and ~30-fold more DHA-containing membrane lipids in the FO-fed versus CO-fed livers and hearts, respectively (Fig 1D-E). Interestingly, this effect was not observed for storage lipids (i.e. triglycerides, TAGs), as DHA did not incorporate into TAGs to a notable extent (not shown).

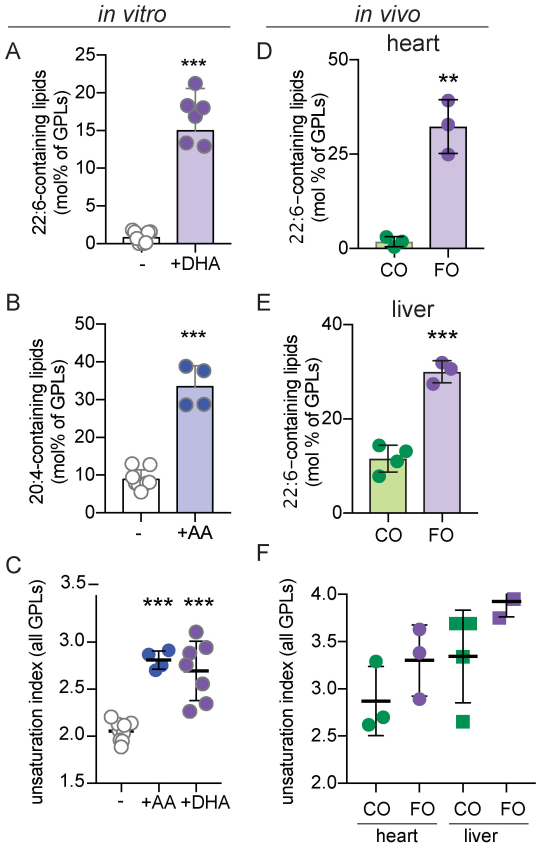

Fig 1. Supplemented PUFAs are robustly and specifically incorporated into membrane phospholipids *in vitro* and *in vivo*. Supplementation of culture media with (A) DHA or (B) AA for 3 days (20 μM) leads to dramatic increase in levels of PUFA-containing membrane lipids in RBL cells, which (C) results in a significant increase in the overall unsaturation of membrane lipids. The unsaturation index is a concentration-weighted average lipid unsaturation. Mice fed diet rich in fish oil (FO) have significantly increased lipids containing DHA in the (D) hearts and (E) livers compared to corn oil (CO) fed. (F) Incorporation of

dietary FAs results in increase in the overall unsaturation of membrane glycerophospholipids (F). Individual experiments (A-C) or animals (D-F) are shown. Bars represent mean ± SD. **p<0.01, ***p<0.001 for student's t-test compared to untreated. Treatment with saturated (PA) or monounsaturated (OA) fatty acids in these conditions had no effect on the lipidome (see Fig S2).

Lipidome remodeling associated with PUFA incorporation

Despite the copious incorporation of exogenous PUFAs into membrane lipids and the resulting increase in overall membrane unsaturation (Fig 1), cells *in vitro* did not show any obvious toxicity or differences in proliferation. This observation was somewhat surprising in light of the central role of lipid unsaturation in membrane physical properties [38,39] and the critical role of those properties in regulating various cellular processes [3,4,7]. Thus, we hypothesized that mammalian cells may compensate for perturbations from exogenous FAs by remodeling their lipidomes. Indeed, while treatments with OA/PA had no effect on overall cell lipidomes (Supp Fig S2; consistent with their lack of incorporation), both AA and DHA supplementation reduced the abundance of other polyunsaturated (i.e. di- and tri-unsaturated) lipid species (Fig 2A-B). This effect could potentially be explained by replacement of these PUFA-containing lipids by AA/DHA-containing ones. Much more surprising was the highly significant increase in fully saturated lipids resulting from PUFA supplementation, due to significantly increased abundance of phospholipid-incorporated saturated fatty acids (Fig 2A-B). We note that for accurate estimates of lipidomic remodeling the supplemented FAs are removed from the analysis (e.g. ω-3-containing lipids from DHA-supplemented data), as the rather extreme over-abundance of those species upon supplementation suppresses the visualization of compensatory effects (original data are shown in Fig S3A). This analysis reveals approximately 2-fold and 4-fold more fully saturated lipids resulting from DHA and AA supplementation, respectively (Fig 2A-B). These changes were associated with significantly reduced overall unsaturation in phospholipids not containing the supplemented FAs (Fig 2A-B, insets). These effects were, at least in part, transcriptionally mediated, as evidenced by mRNA levels of the major fatty acid desaturase enzymes SCD1 and SCD2. As previously reported [40], both were substantially down-regulated by DHA treatment (Fig S4), consistent with more saturated and fewer polyunsaturated lipids. Similar compensatory effects were observed for lipid length. Both AA (20-carbon) and DHA (22-carbon) are relatively long FAs, and thus their incorporation increased the overall length of membrane phospholipids (Fig S3B-C). However, there was also a notable increase in relatively short non-DHA/AA containing lipids (Fig S3D-E). The headgroup profile of membrane lipids was not notably affected by any of the treatments (Supp Fig S3F).

This lipidomic remodeling in response to PUFA feeding *in vitro* was not limited to a single cell type. The observations described so far were on a transformed leukocyte cell line (RBL); however, very similar DHA-induced lipid changes were observed in cultured CHO cells, primary rat hippocampal neurons, primary human MSCs, and MSCs that were differentiated *in vitro* into osteoblasts or adipocytes (Fig. 2C). Remarkably, not only the broad trends of the lipidomic remodeling (more saturated, less unsaturated lipids) were common between these disparate cell lineages and sources, but also the magnitude of the effects were quantitatively similar, despite drastic differences in overall lipid composition [23,34,41,42]. The similarity of the responses between freshly isolated cells, cultured primary cells, and long-term cultured cells lines derived from two different germ layers and three different organisms suggests that comprehensive lipidomic remodeling in response to exogenous PUFAs is a general phenomenon for mammalian cells.

Importantly, we confirmed that this response also occurs *in vivo*. The incorporation of dietary ω-3 PUFAs into mouse heart membrane lipids led to remarkably similar lipidomic remodeling as was observed in cultured cells. Namely, we observed ~3-fold increase in saturated lipids and 50% increased levels of monounsaturated lipids (Fig 2D). Concomitantly, there was a notable reduction in polyunsaturated lipids not containing ω-3 PUFAs. Altogether, the non-ω-3 PUFA lipids were significantly more saturated in heart membranes from FO-fed animals (Fig 2D, inset), fully consistent with compensatory, homeostatic lipidomic remodeling *in vivo*.

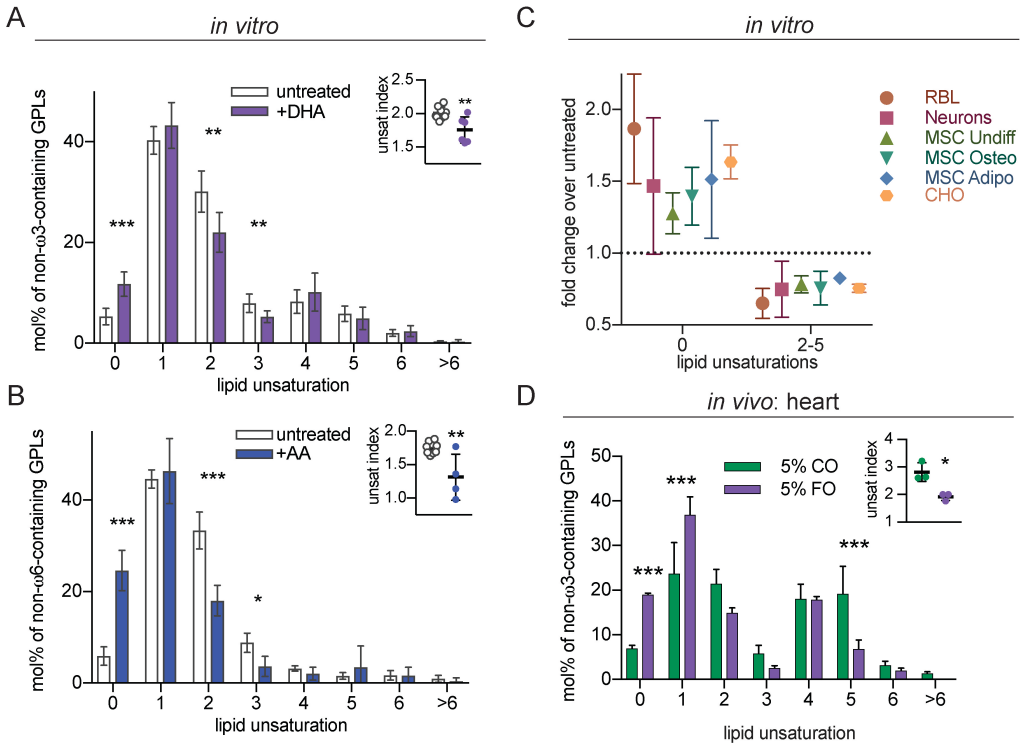

Figure 2 – Lipidome remodeling induced by PUFA supplementation. Lipidome-wide remodeling of lipid unsaturation induced by (A) DHA or (B) AA supplementation. Both PUFAs induce significant upregulation of saturated lipids and downregulation of lipids containing di- and tri-unsaturated lipids. Data shown are for membrane phospholipids not containing the supplemented lipid, i.e. DHA-containing lipids in (A) and AA-containing in (B). Raw lipidomes in Fig S3A show the same trends. (insets) Unsaturation index (concentration-weighted average lipid unsaturation) of non-DHA/AA-containing lipids is significantly reduced upon PUFA supplementation. (C) DHA-mediated lipidomic remodeling, indicated by increased saturated lipids and decreased polyunsaturated lipids (2-5 unsaturations), is consistent across multiple cell types, including isolated rat hippocampal neurons, cultured human MSCs, and MSC differentiated into adipogenic or osteogenic lineages. (D) Lipid unsaturation profiles in membrane lipids isolated from murine heart tissue after feeding with CO versus FO. Incorporation of ω-3 PUFAs into membrane lipids (see Fig 1D) induced robust lipidomic remodeling, increasing saturated and monounsaturated lipids, reducing other PUFA-containing lipids, thereby (inset) decreasing overall unsaturation. All data shown are average +/- SD for n ≥ 3 biological replicates. A, B, and D are two-way ANOVA with Sidak's multiple comparison test. Insets are student's t-test compared to untreated. *p<0.05, **p<0.01, ***p<0.001.

Lipidomic remodeling is nearly concomitant with exogenous PUFA incorporation

The remodeling associated with PUFA incorporation into membrane lipids suggested the induction of a homeostatic membrane response, wherein saturated lipids are upregulated to compensate for the fluidizing effect of PUFA-containing species. To support this inference, we analyzed the temporal profiles of PUFA incorporation and associated lipidomic changes *in vitro*. DHA was rapidly incorporated into membrane lipids, with significant increases in DHA-containing lipids observed within 1 h of supplementation and

half-time of incorporation of ~4 h (Fig 3A-B). The recovery time course was significantly slower, as wash-out of DHA was followed by a return to baseline with a half-time of ~25 h (Fig 3C). This is the approximate doubling time of RBL cells in culture, suggesting that the "wash-out" effect likely results from dilution by new lipid synthesis rather than directed removal of DHA from membrane lipids. Remarkably, the associated lipidome remodeling proceeded with nearly identical temporal profiles to both DHA supplementation and wash-out (Fig 3D-I). The increase in saturated lipids (Fig 3E) and the decrease in di-unsaturated lipids (Fig 3H) were essentially concomitant with DHA incorporation and similar time courses were also observed for the wash-out (Fig 3F and 3I). These observations reveal unexpectedly rapid lipidomic changes to membrane lipid perturbations and suggest that such perturbations induce nearly simultaneous compensatory responses.

The nature of the broad compensatory lipidomic remodeling in response to PUFA supplementation in mammalian cells evokes classical observations of homeoviscous adaptation in ectothermic (e.g. non-thermoregulating) organisms [13-16]. There, perturbations of membrane physical properties produced by changes in ambient temperature are rapidly compensated by lipidomic changes apparently designed to re-normalize membrane physical properties. Our findings suggest that a similar response to fluidizing stimuli occurs in mammalian cells, where it has been co-opted to cope with perturbations from exogenous lipids (e.g. from the diet).

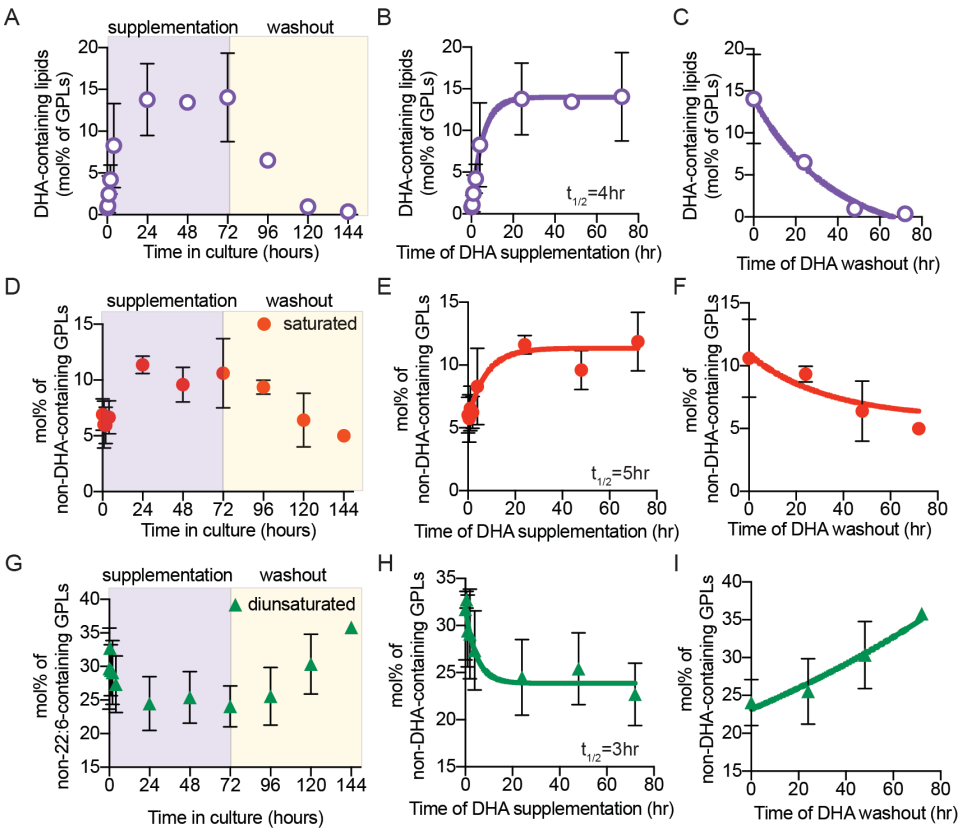

Figure 3 – Time course of DHA incorporation and lipidome remodeling. (A-C) Time course of DHA incorporation into GPLs following supplementation, then wash-out. Time course of concomitant (D-F) saturated lipid and (G-I) di-unsaturated lipid changes induced by DHA supplementation. All data shown are average +/- SD for n ≥ 3 biological replicates.

Cholesterol upregulation by DHA via SREBP2

The above-described acyl chain remodeling in response to PUFA supplementation was incomplete, as the unsaturation index of PUFA-supplemented cells remained higher than those from untreated controls (Fig 1C and 1F). If this lipidome response were designed to normalize membrane properties, the acyl chain remodeling appears insufficient on its own, and there was no remodeling of GPL headgroups. In contrast to most prokaryotes where membrane homeostasis is mediated largely by glycerolipids [14], membrane properties in more complex organisms are regulated to a very significant extent by sterols [43,44]. Thus, we hypothesized that the adaptive response to PUFA perturbation in mammalian cells is also mediated by cholesterol. Indeed, DHA supplementation significantly increased membrane cholesterol over the un-supplemented baseline in both murine heart tissue (Fig 4A) and cultured cells (Fig 4B). In cells, the increase in cholesterol abundance was again quite rapid, with effects observed within 1 h of DHA introduction and reaching a peak after ~4 h (Fig 4C), essentially concomitant with the acyl chain

remodeling (Fig 3). There was also evidence of a small but notable overshoot, as the cholesterol increase was somewhat attenuated after ~4 hrs. These observations suggest that cholesterol upregulation is an early and potent response to membrane perturbation.

The machinery for cholesterol production in metazoans is regulated by proteolytic processing of transcription factors of the sterol regulatory element binding protein (SREBP) family [45]. Specifically, signals to upregulate cellular cholesterol levels are translated into proteolysis of a membrane-bound SREBP2 precursor to release a 'mature' cleaved fragment, which translocates to the nucleus to induce transcription of various target genes, including those for cholesterol synthesis and uptake [45]. Having observed a robust and rapid increase in cholesterol levels resulting from DHA supplementation, we evaluated whether SREBP2 processing was associated with this response. Indeed, DHA feeding increased the production of the 'mature' transcription factor form of SREBP2, with minimal effect on the precursor form (Fig 4D).

These findings suggested that processing of SREBP2 is involved in homeostatic membrane remodeling of mammalian lipid composition in response to perturbation by PUFA incorporation. To test this inference, we measured the response to PUFA supplementation in cells where SREBP processing was inhibited either genetically or pharmacologically. SRD-12B cells are clonal variants of CHO cells wherein a genetic defect in the Site 1 Protease (S1P; cleaves SREBPs to produce the transcriptionally active forms) prevents SREBP processing/activation [46]. In these cells, no notable upregulation of cholesterol (Fig 4E) or saturated lipids (Fig S5) was observed upon DHA supplementation. Similarly, chemical inhibition of SREBP processing by the pentacyclic triterpene betulin [47] completely abrogated DHA-induced upregulation of cholesterol (Fig 4B, triangles) and saturated lipids (Fig S6). These results support the crucial role for SREBP2 in lipidomic remodeling induced by PUFAs.

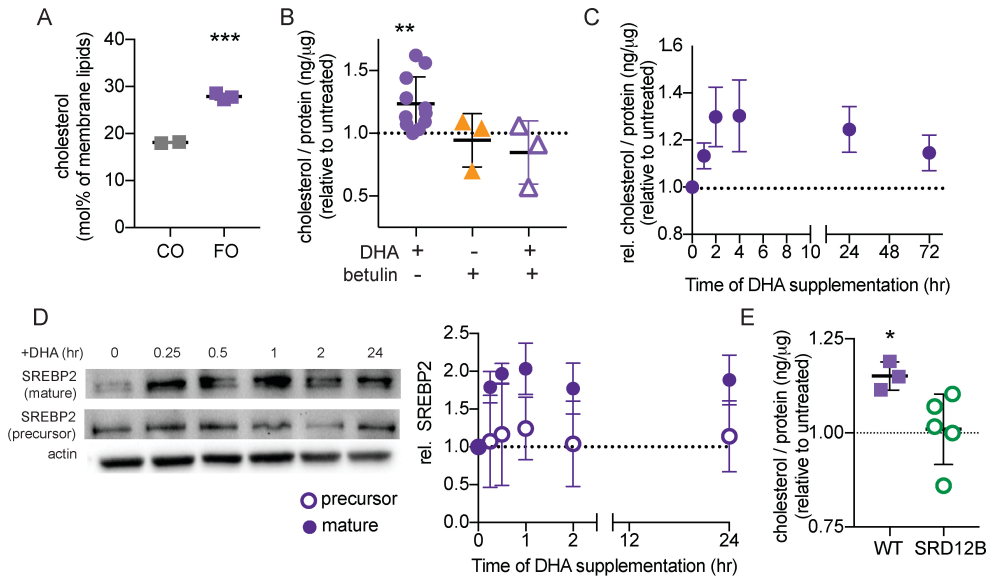

Fig 4 – Cholesterol upregulation by DHA supplementation. (A) Cholesterol is increased in membrane lipids isolated from murine heart tissue after feeding with FO as compared to CO. (B) Membrane cholesterol is significantly increased by DHA supplementation. Cells treated with 200 nM betulin did not upregulate cholesterol upon DHA supplementation. (C) Time course suggests cholesterol increase is a rapid response to DHA-mediated membrane perturbation. (D) The 'mature', transcription-competent form of SREBP2 is rapidly produced in response to DHA supplementation. (E) Cholesterol is significantly increased in WT CHO cells treated with DHA; this effect is abrogated in cells with a defect in SREBP activation (SRD12B; S1P-negative). All data shown are average +/- SD for n ≥ 3 biological replicates; ***p<0.001 in (A) is one-sample t-test between groups; *p<0.05, **p<0.01 in B and E are one-sample t-tests compared to untreated.

Physical homeostasis following lipidomic perturbation

The above data reveal rapid and comprehensive lipidomic remodeling resulting from the incorporation of DHA into membrane lipids, wherein lipids that decrease membrane fluidity / increase membrane packing (saturated lipids and cholesterol) are rapidly upregulated in response to introduction of PUFA-containing lipids that increase membrane fluidity. These changes are consistent with lipidome remodeling for the purpose of homeostatic maintenance of membrane physical properties. To directly evaluate this inference, we measured membrane packing in live cells using a fluorescence assay that relies on a solvatochromic dye (C-Laurdan) whose spectral characteristics are dependent on membrane properties [48]. Specifically, the emission spectrum of C-Laurdan is red-shifted in loosely-packed membranes (due to the enhanced polarity of the fluorophore nano-environment), and the relative extent of this spectral shift can be quantified by ratiometric spectroscopy or imaging [49]. The resulting dimensionless parameter called

Generalized Polarization (GP) is a widely used proxy for membrane packing and fluidity [50-54], with higher values reporting more tightly packed membranes.

Fig 5A shows a map of C-Laurdan GP in live cells generated by confocal spectral imaging [55]. The relatively fluid (low GP; blue/green pixels) internal membranes and relatively packed plasma membranes (high GP; yellow/red pixels) are characteristic of mammalian cells [49,51] (see trace right). These clearly distinct regions enabled us to separately quantify the effects of DHA on plasma versus internal membranes (Fig 5B). The packing of internal membranes was significantly decreased shortly after introduction of exogenous DHA (purple circles; pooled data for 2 and 4 h time points are different from 0 with $p < 0.01$), suggesting reduced packing consistent with the known fluidizing effect of PUFA-containing lipids [23,56]. This response eventually reversed, with GP fully normalizing to baseline by 24 h. Thus, DHA incorporation combined with the associated remodeling produced no net change in overall membrane properties. This renormalization of membrane packing was markedly reduced when lipidomic remodeling was inhibited by targeting SREBP processing. Namely, betulin treatment suppressed the recovery of membrane packing following DHA treatment (Fig. 5B, orange symbols and line), leading to significantly reduced GP in DHA-treated RBL cells after 24 h (Fig. 5B-C). Similarly, while wild-type CHO cells did not show a significant effect of DHA on membrane fluidity after 24 h treatment, DHA supplementation of SRD-12B cells exhibited significantly reduced GP.

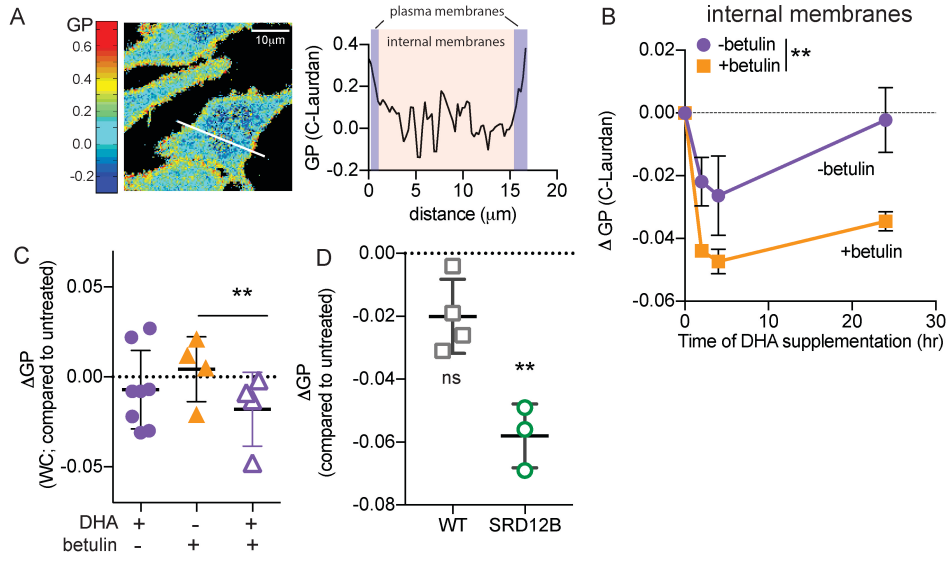

Fig 5 – Physical membrane homeostasis. (A) Exemplary GP map of RBL cells showing the characteristically tighter lipid packing (i.e. greater GP) of the PM compared to internal membranes. (right) line scan of GP across a single cell shown by the white line in the image. (B) Temporal changes in lipid packing (GP) after DHA supplementation and betulin treatment. In control cells, internal membranes initially fluidized by excess DHA-containing lipids (purple) recovered to baseline by 24 hrs. In contrast,

internal membrane packing did not recover in betulin-treated cells (orange). Effect of treatment was significant ($p<0.01$) by 2-way ANOVA; each time point for betulin-treated cells was significantly different from zero ($p<0.01$). (C) Neither DHA or betulin affected membrane packing (GP) alone, whereas cells treated with DHA in the presence of betulin had significantly reduced membrane packing. (D) DHA supplementation of WT CHO cells resulted in no change in membrane packing after 24 h, whereas SRD-12B cells (defective in SREBP processing) had significantly reduced membrane packing. Average +/- SD for $n \geq 3$ biological replicates. ΔGP represent GP of treated cells normalized to untreated cells within each individual experiment. **$p<0.01$ in (C-D) is for one-sample t-tests between groups. **$p<0.05$ in (B) is significance for effect of betulin treatment in 2-way ANOVA.

Disruption of membrane homeostasis reduces cell fitness

In unicellular organisms, the homeoviscous lipidomic response is necessary for maintaining membrane physical properties in a range compatible with the biochemical processes necessary for life [13,15]. Having observed similar lipidomic and biophysical responses in mammalian membranes, we hypothesized that this adaptation was necessary for cellular fitness under conditions of membrane stress. To test this hypothesis, we evaluated the cytological effects of DHA under chemical or pharmacological inhibition of key homeostatic response nodes. Neither DHA nor betulin alone showed significant cytostatic effects; however, DHA supplementation in the presence of betulin led to ~50% decrease in cell number after 3 days of culture (Fig 6A; full dose-response in Supp Fig S7). Similar effects were observed by inhibiting fatty acid synthase (via 10 nM GSK2194069; Fig 6B), which is presumably necessary for production of fatty acids towards the phospholipid remodeling described in Figures 2-3. These observations were confirmed in SRD-12B cells, whose genetic lesion renders them incapable of activating SREBP [46] and mounting an adaptive lipidomic and biophysical response to DHA supplementation (Figs 4E and 5D). Consistent with the abrogated homeostatic response, DHA had a significant cytostatic effect on SRD-12B cells (Fig 6C, green). These results reveal that inhibition of lipidome remodeling in mammalian cells markedly reduced cellular fitness upon membrane perturbation with dietary fatty acids.

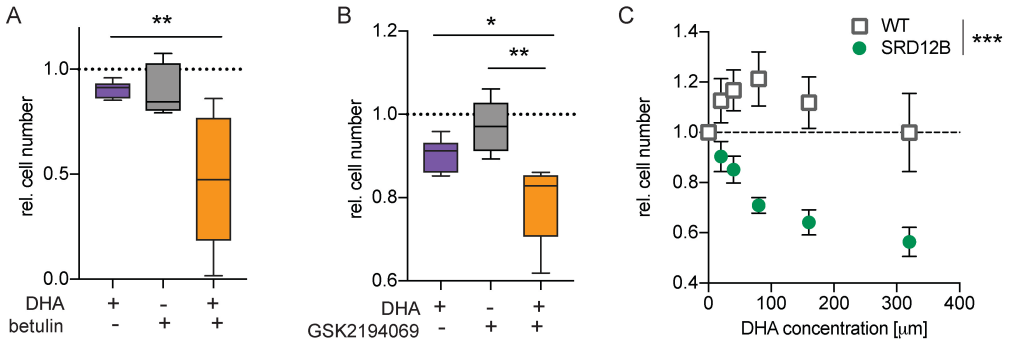

Fig 6 – Inhibition of homeostatic lipidome remodeling reduces cell fitness under DHA supplementation. (A) 200nM betulin completely abrogated DHA-induced upregulation of cholesterol and (B) saturated lipids. (C) Neither DHA nor betulin

alone had a significant effect on cell numbers, whereas the combination was significantly cytostatic. (B) A similar synergistic effect was observed with DHA and GSK2194069 (FAS inhibitor; 10 nM). (C) In SRD-12B cells, which fail to upregulate cholesterol and saturated lipids upon DHA treatment (see Fig 4D and Supp Fig S6), DHA significantly inhibited cell growth, in contrast to control WT CHO cells, wherein DHA showed a slightly mitogenic effect. All data shown as average +/- SD for ≥ 3 independent experiments. A-B are student's t-tests; C is two-way ANOVA for effect of treatment. *p<0.05, **p<0.01, ***p<0.001.

DISCUSSION

The incorporation of dietary fatty acids into mammalian membrane lipids has been widely observed both *in vitro* [23,57,58] and *in vivo* [19,20,36,37,59]. The fact that exogenous fatty acids are so readily used for lipid synthesis is unsurprising in light of the fact that the enzyme required for *de novo* fatty acid production (fatty acid synthase) is minimally expressed in most adult human tissues [60]. Indeed, *de novo* lipogenesis is considered "negligible" [61,62] in adult humans, suggesting that exogenous sources of fatty acids are the major raw material for maintenance and replenishment of membrane lipids. This reliance on exogenous inputs for production of components central to cellular architecture and function would seem to present a major complication for homeostasis.

In ectothermic organisms, homeostatic membrane control has been widely observed in the form of homeoviscous adaptation [13-15]. According to this hypothesis, the relative abundance of saturated to unsaturated membrane lipids is responsive to temperatures changes in order to maintain membrane fluidity at the level required for the many processes hosted and regulated by cell membranes. Although such adaptation has been proposed in prokaryotes [14], single-celled eukaryotes [63], and even cold-blooded animals [64,65], studies on endothermic organisms have been limited [28,29], and there has yet been no direct observations of HVA in mammals or isolated mammalian cells. Our data directly confirm the three major tenets of cell-autonomous homeoviscous adaptation: (1) lipidomic remodeling resulting from a perturbation of membrane physical properties (Fig 2-4); (2) recovery of baseline physical properties at a new lipid composition (Fig 5); and (3) necessity of this response for cellular fitness (Fig 6). These observations suggest that mammalian cells possess the capacity for homeostatic membrane adaptation analogous to HVA, and that this response can compensate for perturbations from dietary lipid inputs.

In cold-blooded animals, the homeostatic membrane response also involves modulation of cholesterol levels [44,65], and we observe a similar response in mammalian cells, mediated at least partially through activation of SREBP2 (Fig 4). It is quite remarkable to note that disruption of SREBP activation either by betulin or in SRD-12B cells resulted in near-complete abrogation of the compensatory response. This abrogation was notable not only in the lack of cholesterol upregulation (Fig 4D and 6A), which may have

been expected, but also in the failure to upregulate saturated lipids (Figs S5 and S6), a response not directly connected to SREBP2 target genes.

Our implication of SREBP2 as a critical node of the sense-and-respond module for membrane adaptation is consistent with the central role of SREBPs in membrane homeostasis [45]. SREBP transcription factors have been dubbed the "master regulators of lipid homeostasis", because they direct not only cholesterol synthesis and uptake, but also proteins associated with membrane lipid metabolism, including those involved in FA synthesis, elongation, and desaturation [66]. The effect of PUFA supplementation on SREBP function has been extensively studied, and DHA is known to suppress the activation of SREBP1 and its target genes, both in cultured cells and *in vivo* [67-69]. We observed downregulation of two SREBP1 target genes (SCD1 and SCD2, Fig S3) suggesting a similar effect in our cells. In contrast, SREBP2 is not suppressed by PUFAs [67,68], revealing that these two complementary regulators of membrane homeostasis have different functions, despite both being sensitive to membrane cholesterol. In our observations, SREBP2 is induced as a necessary part of the homeostatic response. Previous reports [68] have not noted a significant effect of PUFAs on SREBP2, possibly because those experiments involved acute PUFA feeding of serum-starved cells, where high levels of activated SREBPs may have suppressed the DHA-mediated stimulation we observe here. We have confirmed this effect in our cells (not shown). It remains to be determined whether SREBP2 is simply an effector of membrane remodeling downstream of yet-unidentified sensing machinery, or whether this protein (and/or its regulatory machinery) may itself be capable of sensing perturbations in membrane physical properties. Direct demonstration of protein responsiveness to membrane packing has recently been described for two yeast ER proteins [5,18], providing a conceptual and methodological toolbox for identifying other membrane sensors. Remarkably, despite the ubiquity and importance of membrane homeostasis, the machinery used for sensing membrane properties remains largely uncharacterized. It is an intriguing observation that Ire1, a core component of the unfolded protein response (UPR), exhibits a dual sensitivity to unfolded proteins and aberrant lipid compositions, demonstrating a tight connection between protein-folding and membrane properties [18]. This connection suggests that the machinery for ameliorating protein-folding stresses may also be involved in transducing and mitigating membrane stress [70].

In summary, our observations strongly support the hypothesis that mammalian cells in culture and *in vivo* sense membrane physical properties and respond to perturbations by comprehensive remodeling of their lipidomes. In our measurements, the perturbations were induced by supplementation with polyunsaturated fatty acids (PUFAs); however, it is likely that other fats (e.g. cholesterol) or amphiphiles (bile acids, anesthetics) may induce similar responses. We implicate SREBP2 as a central response mediator and show

that the compensatory response is important for cell fitness, confirming membrane adaptation as a central requirement for cellular homeostasis.

MATERIALS AND METHODS

Materials: Betulin and GSK2194069 were obtained from Sigma Aldrich. C-Laurdan was purchased from TPProbes (South Korea). Amplex Red kit to quantify cholesterol was purchased from Invitrogen. Antibodies used: actin (monoclonal clone AC-15, Abcam), SREBP2 (polyclonal, Abcam).

Cell culture: Rat basophilic leukemia (RBL) cells were maintained in medium containing 60% modified Eagle's medium (MEM), 30% RPMI, 10% fetal calf serum, 100 units/mL penicillin, and 100 µg/mL streptomycin. Chinese hamster ovary (CHO) cells were maintained in DMEM:F12 (1:1) containing 5% fetal calf serum, 100 units/mL penicillin, and 100 µg/mL streptomycin. SRD12B cells were maintained in DMEM:F12 (1:1) containing 5% fetal calf serum, 50µM sodium mevalonate, 20µM oleic acid, 5µg/mL cholesterol, 100 units/mL penicillin, and 100 µg/mL streptomycin. All cells were grown at 37ºC in humidified 5% CO2.

Fatty acid treatments: Fatty acid stock solutions were received as air-purged ampules (Sigma Aldrich) and loaded into BSA immediately upon opening. BSA loading was accompanied by stirring the fatty acid with BSA dissolved in water (2:1 mol/mol FA:BSA), sterile filtering, purging with nitrogen prior to aliquoting, and storing at -80°C. BSA loading, purging, and cold storage were all done to minimize FA oxidation. For all experiments with FA supplementation, cells were incubated with 20 µM FA for 3 days (cells were re-supplemented 24 h prior to analysis). Serum-containing, rather than serum-free, media was used to approximate physiological supplementation, rather than exclusive introduction of specific FAs. These conditions were chosen to approximate *in vivo* settings produced by DHA-enriched diets in mammals: plasma free FA concentrations range from 300 to 750 µM [59,71] and up to 10 mol % of plasma fatty acids are ω-3 DHA in rats fed a high-fish-oil diet [59]. Further, diets rich in ω-3 PUFAs led to significant incorporation of these fats into cell membrane lipids [19,37,59], similar to the levels we observed under our culture feeding conditions (Fig. 1). For these reasons, we believe our culture conditions reasonably approximate physiological dietary membrane perturbations.

Animals and diets: All experimental procedures using laboratory animals were approved by the University Laboratory Animal Care Committee of Texas A&M University. Pathogen-free female C57BL/6 mice (n=180; Frederick Research Facility, Frederick, MD) weighing 16–18 g, were randomly

425 divided into two groups of 90. For 2 wk, mice had free access to one of the two semipurified diets, which
426 were adequate in all nutrients [35]. Diets varied only in the oil composition, i.e., either corn oil (CO) or an
427 (n-3) PUFA-enriched fish-corn oil (FO) mixture (4:1, w/w) at 5 g/100 g diet. The basic diet composition,
428 expressed as g/100 g was: casein, 20; sucrose, 42; cornstarch, 22; cellulose, 6; AIN-76 mineral mix, 3.5;
429 AIN-76 vitamin mix, 1, DL-methionine, 0.3; choline chloride, 0.2; Tenox 20A (containing 32% glycerol,
430 30% corn oil, 20% tert-butylhydroquinone, 15% propylene glycol, 3% citric acid) 0.1; and oil, 5. The fatty
431 acid composition of the diets, as determined by gas chromatography, is shown in Supplemental Table 1.
432 Mice were killed by CO2 asphyxiation after two weeks of feeding the CO/FO diet, and the livers and
433 hearts were isolated and frozen in liquid nitrogen. 20-50 mg of tissue was mechanically homogenized in
434 Dulbecco's PBS (without Ca^{2+} and Mg^{2+}). Samples were further diluted to 5 mg/mL in Dulbecco's PBS
435 (without Ca^{2+} and Mg^{2+}), and lipidomics analysis was performed as below.

436 ***Drug treatments and cell number quantification:*** RBL cells were treated with or without 20 μM DHA
437 in the presence or absence of betulin (inhibitor of SREBP processing) or GSK2194069 (FAS inhibitor).
438 Cells were treated for 72 h and then the cell number determined via fluorescein diacetate (FDA)
439 fluorescence. FDA is a cell viability probe which freely diffuses through cell membranes, but is trapped
440 in cells following de-acytelation by cytoplasmic esterases in viable cells. The number of viable cells is
441 then directly related to fluorescein fluorescence intensity. For the assay, cells were treated in 96-well
442 plates, gently washed with PBS, and then incubated with fluorescein diacetate (5 μg/mL in PBS) for 2
443 minutes at 37°C. The plates were then washed again to remove excess FDA and fluorescence was
444 measured at 488 nm excitation and 520 nm emission. For each experiment the number of cells per well
445 were normalized to untreated, unsupplemented cells.

446 ***Lipidomics:*** Detailed lipidomic analysis was performed by Lipotype, GmbH, as previously described[72].
447 Briefly, for preparation of crude cell membranes, cells were washed with phosphate buffered saline (PBS),
448 scraped in 10 mM Tris pH 7.4, and then homogenized with a 27-gauge needle. Nuclei were then pelleted
449 by centrifugation at 300 xg for 5 min. The supernatant was pelleted by centrifugation at 100,000 xg for 1
450 h at 4°C. The membrane pellet was then washed and resuspended in 150 mM ammonium bicarbonate.

451 *Lipids detected*: ceramide (Cer), Chol, SM, diacylglycerol (DAG), lactosyl ceramide (DiHexCer),
452 glucosyl/galactosyl ceramide (HexCer), sterol ester (SE), and triacylglycerol (TAG), as well as
453 phosphatidic acid (PA), phosphatidylcholine (PC), phosphatidylethanolamine (PE), phosphatidylglycerol
454 (PG), and phosphatidylinositol (PI), phosphatidylserine (PS), and their respective lysospecies (lysoPA,
455 lysoPC, lysoPE, lysoPI, and lysoPS) and ether derivatives (PC O-, PE O-, LPC O-, and LPE O-). Lipid

456 species were annotated according to their molecular composition as follows: [lipid class]-[sum of carbon
457 atoms in the FAs]:[sum of double bonds in the FAs];[sum of hydroxyl groups in the long chain base and
458 the FA moiety] (e.g., SM-32:2;1). When available, the individual FA composition according to the same
459 rule is given in brackets (e.g., 18:1;0-24:2;0)

460 *Lipid extraction*: Samples were extracted and analyzed as previously described (39,47), which is a
461 modification of a previously published method for shotgun lipidomics (48). Briefly, membrane samples
462 were suspended in 150 µL of 150 mM ammonium bicarbonate in water, spiked with 20 µL of internal
463 standard lipid mixture, and then extracted with 750 µL of a chloroform/methanol 10:1 (v/v) mixture for 2
464 h at 4_C with 1400 rpm shaking. After centrifugation (3 min, 3000 **g**) to facilitate phase partitioning, the
465 lower, lipid-containing, organic phase was collected (first-step extract), and the remaining water phase
466 was further extracted with 750 µL of a chloroform/methanol 2:1 (v/v) mixture under the same conditions.
467 Again the lower, organic phase was collected (second-step extract). Extracts were dried in a speed vacuum
468 concentrator, and 120 µL of a dried first-step extract underwent acetylation with 75 µL of an acetyl
469 chloride/chloroform 1:2 (v/v) mixture for 1 h to derivatize Chol. After the reaction was completed, the
470 mixture was dried. Then, 120 µL of a dried first-step extract and a derivatized extract were resuspended
471 in an acquisition mixture with 8 mM ammonium acetate (400 mM ammonium acetate in
472 methanol/chloroform/methanol/propan-2-ol, 1:7:14:28, v/v/v/v). Next, 120 µL of the second-step extract
473 was resuspended in an acquisition mixture with 30 µL 33% methylamine in methanol, in 60 mL
474 methanol/chloroform 1:5 (v/v). All liquid-handling steps were performed using a Hamilton (Reno, NV)
475 STARlet robotic platform with the Anti Droplet Control feature, ensuring the accuracy and reproducibility
476 of organic solvent pipetting.

477 *Lipid standards*: Synthetic lipid standards were purchased from Sigma-Aldrich (Chol D6), Larodan
478 (Solna, Sweden) Fine Chemicals (DAG and TAG), and Avanti Polar Lipids (all others). The standard lipid
479 mixtures were chloroform/ methanol 1:1 (v/v) solutions containing Cer 35:1;2, (D18:1;2, 17:0;0); Chol
480 D6; DAG 34:0;0 (17:0;0, 17:0;0); DiHexCer 30:1;2 (D18:1;2.12:0;0); HexCer 30:1;2 (D18:1;2.12:0;0);
481 LPA 17:0;0 (17:0;0); LPC 12:0;0 (12:0;0); LPE 17:1;0 (17:1;0); LPI 17:1;0 (17:1;0); LPS 17:1;0 (17:1;0);
482 PA 34:0;0 (17:0;0, 17:0;0); PC 34:0;0 (17:0;0, 17:0;0); PE 34:0;0 (17:0;0, 17:0;0); PG 34:0;0 (17:0;0,
483 17:0;0); PI 32:0;0 (16:0;0, 16:0;0); PS 34:0;0 (17:0;0, 17:0;0); SE 20:0;0 (20:0;0); SM 30:1;2 (18:1;2,
484 12:0;0); and TAG 51:0;0 (17:0;0, 17:0;0, 17:0;0).

485 *Lipid spectrum acquisition:* Extracts in the acquisition mixtures were infused with a robotic nanoflow ion
486 source (TriVersa NanoMate; Advion Biosciences, Ithaca, NY) into a mass spectrometer instrument (Q

Exactive, Thermo Scientific). Cer, DiHexCer, HexCer, lysolipids, and SM were monitored by negative ion mode Fourier transform mass spectrometry (FT-MS). PA, PC, PE, PI, PS, and ether species were monitored by negative ion mode FT tandem MS (FT-MS/MS). Acetylated Chol was monitored by positive ion mode FTMS. SE, DAG, TAG, and species were monitored by positive ion mode FT-MS/MS.

Lipid identification and quantification: Automated processing of acquired mass spectra, and identification and quantification of detected molecular lipid species were performed with the use of LipidXplorer software (17). Only lipid identifications with a signal/noise ratio of >5, an absolute abundance of at least 1 pmol, and a signal intensity fivefold higher than in the corresponding blank samples were considered for further data analysis.

C-laurdan spectroscopy: Membrane packing (related to order and fluidity) was determined via C-laurdan spectroscopy as described [73,74]. Briefly, cells were washed with PBS and stained with 20 μg/mL C-laurdan for 10 minutes on ice. The emission spectrum from isolated GPMVs was gathered from 400-550 nm with excitation at 385 nm at 23°C. The GP was calculated according to the following equation:

$$GP = \frac{\sum_{420}^{460} I_x - \sum_{470}^{510} I_x}{\sum_{420}^{460} I_x + \sum_{470}^{510} I_x}$$

C-Laurdan spectral imaging: C-Laurdan imaging was performed as previously described [23,34,55,73,74]. Briefly, cells were washed with PBS and stained with 10 μg/mL C-Laurdan for 10 min on ice, then imaged via confocal microscopy on a Nikon A1R with spectral imaging at 60x and excitation at 405 nm. The emission was collected in two bands: 433–463 nm and 473–503 nm. MATLAB (MathWorks, Natick, MA) was used to calculate the two-dimensional (2D) GP map, where GP for each pixel was calculated from a ratio of the two fluorescence channels, as previously described [55]. Briefly, each image was binned (2x2), background subtracted, and thresholded to keep only pixels with intensities greater than 3 standard deviations of the background value in both channels. The GP image was calculated for each pixel using the above equation. GP maps (pixels represented by GP value rather than intensity) were imported into ImageJ. Line scans were drawn across individual cells. PM GP values were calculated as averages of the peaks as values higher than 0.26. For internal membranes, average GP values were calculated from line scans around the nucleus (visible as a dark spot in C-Laurdan images). At least 10 cells were imaged and quantified per experiment with at least 4 individual experiments performed. Reported are the mean and standard deviations of the average GP values for the individual experiments.

Amplex Red assay: Amplex Red cholesterol assay was performed (according to manufacturer instructions; Invitrogen) to determine the abundance of cholesterol. Each reading was normalized to protein concentration (determined by bicinchoninic acid (BCA) assay) in the same samples. Technical triplicates were measured for each sample. Shown are values normalized to untreated cells. Reported are the average and standard deviations from at least 3 independent biological replicates.

Western Blot: Cells were washed with ice cold PBS, then scraped into Laemmli lysis buffer (50mM Tris-HCl, pH 8.0; 2% SDS; 5mM EDTA, pH8.0) supplemented with protease inhibitor cocktail. Protein concentration was determined using BCA (Pierce), and equal amounts of protein were mixed with reducing Laemmli sample buffer and loaded onto SDS-PAGE gels. Gels were transferred to PVDF membranes, which were blocked in 5% BSA. Membranes were incubated with primary antibodies overnight at 4°C, and detected with either AlexaFluor or HRP-tagged secondary antibodies. Membranes were imaged using a BioRad ChemiDoc imager. The intensities of the bands were quantified normalized to actin, and plotted as mean ± SD of $n \geq 3$ experiments.

Real Time Quantitative PCR: Total RNA was isolated via Trizol (Sigma) following the manufacturer's protocol. Reverse transcriptase PCR was performed using the High Capacity cDNA Reverse Transcription Kit from Applied Biosystems according to manufacturer's protocol. To quantify mRNA expression, SYBR Fast MasterMix (2x) Universal Dye (#KK4602) from Kapa Biosystems was used in an Eppendorf Realplex2 Mastercycler. Each primer set for each sample was run in triplicate with 1 ng of cDNA per well. The primer sets used are:

Gene	Forward Primer	Reverse Primer
GAPDH	GTCTACTGGCGTCTTCACCA	GTGGCAGTGATGGCATGGAC
SCD1	GTGATGTTCCAGAGGAGGTACT	CAGGAACTCAGAAGCCCAGAA
SCD2	GGTGATGTTCCAGAGGAGGTATT	AACTGGAAGACCCCGAACTC

Expression changes were calculated using the delta delta C_T method. The data was standardized using a previously published protocol [75] in which the average fold change was log transformed, mean centered, and confidence intervals determined to evaluate statistical significance.

Acknowledgements

All confocal microscopy was performed at the Center for Advanced Microscopy, Department of Integrative Biology and Pharmacology McGovern Medical School at the University of Texas Health Science Center at Houston. We acknowledge funding from the Cancer Prevention Research Institute of Texas (CPRIT; R1215), NIH/National Institute of General Medical Sciences (grant nos. GM114282, GM124072, GM120351), and the Volkswagen Foundation (grant no. 93091).

References

1 Krogh, A., Larsson, B., von Heijne, G. & Sonnhammer, E. L. Predicting transmembrane protein topology with a hidden Markov model: application to complete genomes. *Journal of molecular biology* **305**, 567-580, (2001).

2 Janmey, P. A. & Kinnunen, P. K. Biophysical properties of lipids and dynamic membranes. *Trends in cell biology* **16**, 538-546, (2006).

3 Los, D. A. & Murata, N. Membrane fluidity and its roles in the perception of environmental signals. *Biochim Biophys Acta* **1666**, 142-157, (2004).

4 Andersen, O. S. & Koeppe, R. E., 2nd. Bilayer thickness and membrane protein function: an energetic perspective. *Annu Rev Biophys Biomol Struct* **36**, 107-130, (2007).

5 Covino, R. *et al.* A eukaryotic sensor for membrane lipid saturation. *Molecular cell* **63**, 49-59, (2016).

6 daCosta, C. J., Dey, L., Therien, J. P. & Baenziger, J. E. A distinct mechanism for activating uncoupled nicotinic acetylcholine receptors. *Nat Chem Biol* **9**, 701-707, (2013).

7 Marsh, D. Protein modulation of lipids, and vice-versa, in membranes. *Biochim Biophys Acta* **1778**, 1545-1575, (2008).

8 Roux, A. *et al.* Membrane curvature controls dynamin polymerization. *Proc Natl Acad Sci U S A* **107**, 4141-4146, (2010).

9 Shi, Z. & Baumgart, T. Membrane tension and peripheral protein density mediate membrane shape transitions. *Nature communications* **6**, 5974, (2015).

10 Rosholm, K. R. *et al.* Membrane curvature regulates ligand-specific membrane sorting of GPCRs in living cells. *Nat Chem Biol* **13**, 724-729, (2017).

11 Sezgin, E., Levental, I., Mayor, S. & Eggeling, C. The mystery of membrane organization: composition, regulation and roles of lipid rafts. *Nat Rev Mol Cell Biol* **18**, 361-374, (2017).

12 Lorent, J. H. *et al.* Structural determinants and functional consequences of protein affinity for membrane rafts. *Nature communications* **8**, 1219, (2017).

13 Hazel, J. R. Thermal adaptation in biological membranes: is homeoviscous adaptation the explanation? *Annu Rev Physiol* **57**, 19-42, (1995).

14 Sinensky, M. Homeoviscous adaptation--a homeostatic process that regulates the viscosity of membrane lipids in Escherichia coli. *Proc Natl Acad Sci U S A* **71**, 522-525, (1974).

15 Ernst, R., Ejsing, C. S. & Antonny, B. Homeoviscous adaptation and the regulation of membrane lipids. *Journal of molecular biology* **428**, 4776-4791, (2016).

16 Guschina, I. A. & Harwood, J. L. Mechanisms of temperature adaptation in poikilotherms. *FEBS Lett* **580**, 5477-5483, (2006).

17 Aguilar, P. S. *et al.* Molecular basis of thermosensing: a two-component signal transduction thermometer in Bacillus subtilis. *EMBO J* **20**, 1681-1691, (2001).

18 Halbleib, K. *et al.* Activation of the unfolded protein response by lipid bilayer stress. *Molecular cell* **67**, 673-684 e678, (2017).

19 Cao, J., Schwichtenberg, K. A., Hanson, N. Q. & Tsai, M. Y. Incorporation and clearance of omega-3 fatty acids in erythrocyte membranes and plasma phospholipids. *Clinical chemistry* **52**, 2265-2272, (2006).

20 Oliveira, T. V. *et al.* Impact of high cholesterol intake on tissue cholesterol content and lipid transfers to high-density lipoprotein. *Nutrition* **27**, 713-718, (2011).

21 Gerl, M. J. *et al.* Quantitative analysis of the lipidomes of the influenza virus envelope and MDCK cell apical membrane. *J Cell Biol* **196**, 213-221, (2012).

22 Sampaio, J. L. *et al.* Membrane lipidome of an epithelial cell line. *Proc Natl Acad Sci U S A* **108**, 1903-1907, (2011).

23 Levental, K. R. *et al.* Polyunsaturated lipids regulate membrane domain stability by tuning membrane order. *Biophys J* **110(8)**, 1800-1810, (2016).

24 Han, X. in *Lipidomics* 427-442 (John Wiley & Sons, Inc, 2016).

25 Klemm, R. W. *et al.* Segregation of sphingolipids and sterols during formation of secretory vesicles at the trans-Golgi network. *J Cell Biol* **185**, 601-612, (2009).

26 Ejsing, C. S. *et al.* Global analysis of the yeast lipidome by quantitative shotgun mass spectrometry. *Proc Natl Acad Sci U S A* **106**, 2136-2141, (2009).

27 Sinensky, M. Defective regulation of cholesterol biosynthesis and plasma membrane fluidity in a Chinese hamster ovary cell mutant. *Proc Natl Acad Sci U S A* **75**, 1247-1249, (1978).

28 Sinensky, M. Adaptive alteration in phospholipid composition of plasma membranes from a somatic cell mutant defective in the regulation of cholesterol biosynthesis. *J Cell Biol* **85**, 166-169, (1980).

29 Dymond, M. K. Mammalian phospholipid homeostasis: homeoviscous adaptation deconstructed by lipidomic data driven modelling. *Chem Phys Lipids* **191**, 136-146, (2015).

30 Dymond, M. K., Hague, C. V., Postle, A. D. & Attard, G. S. An in vivo ratio control mechanism for phospholipid homeostasis: evidence from lipidomic studies. *J R Soc Interface* **10**, 20120854, (2013).

31 Sodt, A. J., Venable, R. M., Lyman, E. & Pastor, R. W. Nonadditive Compositional Curvature Energetics of Lipid Bilayers. *Phys Rev Lett* **117**, 138104, (2016).

32 Almeida, P. F. Thermodynamics of lipid interactions in complex bilayers. *Biochim Biophys Acta* **1788**, 72-85, (2009).

33 Balogh, G. *et al.* Key role of lipids in heat stress management. *FEBS Lett* **587**, 1970-1980, (2013).

34 Levental, K. R. *et al.* omega-3 polyunsaturated fatty acids direct differentiation of the membrane phenotype in mesenchymal stem cells to potentiate osteogenesis. *Science advances* **3**, eaao1193, (2017).

35 Fan, Y. Y., McMurray, D. N., Ly, L. H. & Chapkin, R. S. Dietary (n-3) polyunsaturated fatty acids remodel mouse T-cell lipid rafts. *The Journal of nutrition* **133**, 1913-1920, (2003).

36 Stark, K. D. *et al.* Fatty acid compositions of serum phospholipids of postmenopausal women: a comparison between Greenland Inuit and Canadians before and after supplementation with fish oil. *Nutrition* **18**, 627-630, (2002).

37 Metcalf, R. G. *et al.* Effects of fish-oil supplementation on myocardial fatty acids in humans. *The American journal of clinical nutrition* **85**, 1222-1228, (2007).

38 van Blitterswijk, W. J., van der Meer, B. W. & Hilkmann, H. Quantitative contributions of cholesterol and the individual classes of phospholipids and their degree of fatty acyl (un)saturation to membrane fluidity measured by fluorescence polarization. *Biochemistry* **26**, 1746-1756, (1987).

39 Lande, M. B., Donovan, J. M. & Zeidel, M. L. The relationship between membrane fluidity and permeabilities to water, solutes, ammonia, and protons. *J Gen Physiol* **106**, 67-84, (1995).

40 Sessler, A. M., Kaur, N., Palta, J. P. & Ntambi, J. M. Regulation of stearoyl-CoA desaturase 1 mRNA stability by polyunsaturated fatty acids in 3T3-L1 adipocytes. *J Biol Chem* **271**, 29854-29858, (1996).

41 Levental, I. & Veatch, S. L. The continuing mystery of lipid rafts. *J. Mol. Biol.* **428**, 4749-4764, (2016).

42 Lin, X. *et al.* Domain stability in biomimetic membranes driven by lipid polyunsaturation. *J Phys Chem B* **120**, 11930-11941, (2016).

43 Yeagle, P. L. Cholesterol and the cell membrane. *Biochim Biophys Acta* **822**, 267-287, (1985).

44 Crockett, E. Cholesterol Function in Plasma Membranes from Ectotherms: Membrane-Specific Roles in Adaptation to Temperature. *Integrative and Comparative Biology* **38**, 298-304, (1998).

45 Raghow, R. *et al.* SREBPs: the crossroads of physiological and pathological lipid homeostasis. *Trends Endocrinol Metab* **19**, 65-73, (2008).

46 Sakai, J. *et al.* Molecular identification of the sterol-regulated luminal protease that cleaves SREBPs and controls lipid composition of animal cells. *Molecular cell* **2**, 505-514, (1998).

47 Tang, J. J. *et al.* Inhibition of SREBP by a small molecule, betulin, improves hyperlipidemia and insulin resistance and reduces atherosclerotic plaques. *Cell Metab* **13**, 44-56, (2011).

48 Kim, H. M. *et al.* A two-photon fluorescent probe for lipid raft imaging: C-laurdan. *Chembiochem* **8**, 553-559, (2007).

49 Owen, D. M. *et al.* Quantitative imaging of membrane lipid order in cells and organisms. *Nat Protoc* **7**, 24-35, (2011).

50 Kaiser, H. J. *et al.* Order of lipid phases in model and plasma membranes. *Proc Natl Acad Sci U S A* **106**, 16645-16650, (2009).

51 Gaus, K. *et al.* Condensation of the plasma membrane at the site of T lymphocyte activation. *J Cell Biol* **171**, 121-131, (2005).

52 Parasassi, T. *et al.* Quantitation of lipid phases in phospholipid vesicles by the generalized polarization of Laurdan fluorescence. *Biophys J* **60**, 179-189, (1991).

53 Sezgin, E. *et al.* Adaptive lipid packing and bioactivity in membrane domains. *PloS one* **10**, e0123930, (2015).

54 Levental, K. R. & Levental, I. Giant plasma membrane vesicles: models for understanding membrane organization. *Current topics in membranes* **75**, 25-57, (2015).

55 Sezgin, E., Waithe, D., Bernardino de la Serna, J. & Eggeling, C. Spectral imaging to measure heterogeneity in membrane lipid packing. *Chemphyschem* **16**, 1387-1394, (2015).

56 Feller, S. E., Gawrisch, K. & MacKerell, A. D., Jr. Polyunsaturated fatty acids in lipid bilayers: intrinsic and environmental contributions to their unique physical properties. *J Am Chem Soc* **124**, 318-326, (2002).

57 Briolay, A., Jaafar, R., Nemoz, G. & Bessueille, L. Myogenic differentiation and lipid-raft composition of L6 skeletal muscle cells are modulated by PUFAs. *Biochim Biophys Acta* **1828**, 602-613, (2013).

58 Seo, J. *et al.* Docosahexaenoic acid selectively inhibits plasma membrane targeting of lipidated proteins. *FASEB journal : official publication of the Federation of American Societies for Experimental Biology* **20**, 770-772, (2006).

59 Yaqoob, P. *et al.* Comparison of the effects of a range of dietary lipids upon serum and tissue lipid composition in the rat. *The international journal of biochemistry & cell biology* **27**, 297-310, (1995).

60 Kusakabe, T. *et al.* Fatty acid synthase is expressed mainly in adult hormone-sensitive cells or cells with high lipid metabolism and in proliferating fetal cells. *J Histochem Cytochem* **48**, 613-622, (2000).

61 Weiss, L. *et al.* Fatty-acid biosynthesis in man, a pathway of minor importance. Purification, optimal assay conditions, and organ distribution of fatty-acid synthase. *Biol Chem Hoppe Seyler* **367**, 905-912, (1986).

62 Murphy, E. J. Stable isotope methods for the in vivo measurement of lipogenesis and triglyceride metabolism. *J Anim Sci* **84 Suppl**, E94-104, (2006).

63 Nakagawa, Y., Sakumoto, N., Kaneko, Y. & Harashima, S. Mga2p is a putative sensor for low temperature and oxygen to induce OLE1 transcription in Saccharomyces cerevisiae. *Biochem Biophys Res Commun* **291**, 707-713, (2002).

64 Tiku, P. E. *et al.* Cold-induced expression of delta 9-desaturase in carp by transcriptional and posttranslational mechanisms. *Science* **271**, 815-818, (1996).

65 Burns, M. *et al.* Miscibility Transition Temperature Scales with Growth Temperature in a Zebrafish Cell Line. *Biophys J* **113**, 1212-1222, (2017).

66 Eberle, D. *et al.* SREBP transcription factors: master regulators of lipid homeostasis. *Biochimie* **86**, 839-848, (2004).

67 Yahagi, N. *et al.* A crucial role of sterol regulatory element-binding protein-1 in the regulation of lipogenic gene expression by polyunsaturated fatty acids. *J Biol Chem* **274**, 35840-35844, (1999).

68 Hannah, V. C. *et al.* Unsaturated fatty acids down-regulate srebp isoforms 1a and 1c by two mechanisms in HEK-293 cells. *J Biol Chem* **276**, 4365-4372, (2001).

69 Xu, J. *et al.* Polyunsaturated fatty acids suppress hepatic sterol regulatory element-binding protein-1 expression by accelerating transcript decay. *J Biol Chem* **276**, 9800-9807, (2001).

70 Radanovic, T. *et al.* An Emerging Group of Membrane Property Sensors Controls the Physical State of Organellar Membranes to Maintain Their Identity. *BioEssays : news and reviews in molecular, cellular and developmental biology*, e1700250, (2018).

71 Pirro, M. *et al.* Plasma free fatty acid levels and the risk of ischemic heart disease in men: prospective results from the Quebec Cardiovascular Study. *Atherosclerosis* **160**, 377-384, (2002).

72 Tulodziecka, K. *et al.* Remodeling of the postsynaptic plasma membrane during neural development. *Mol Biol Cell* **27**, 3480-3489, (2016).

73 Sezgin, E. *et al.* Elucidating membrane structure and protein behavior using giant plasma membrane vesicles. *Nat Protoc* **7**, 1042-1051, (2012).

74 Levental, K. R. & Levental, I. Isolation of giant plasma membrane vesicles for evaluation of plasma membrane structure and protein partitioning. *Methods in molecular biology* **1232**, 65-77, (2015).

75 Willems, E., Leyns, L. & Vandesompele, J. Standardization of real-time PCR gene expression data from independent biological replicates. *Analytical biochemistry* **379**, 127-129, (2008).